

Flow separation in laminar natural convection

K. Gersten,* M. Grobel,† H. Klick* and W. Merzkirch†

*Institut für Thermo- und Fluidodynamik, Universität Bochum, Germany

†Lehrstuhl für Strömungslehre, Universität Essen, Germany

Theoretical and experimental studies of flow separation in laminar natural convection are presented. Since classical boundary-layer theory cannot determine separation on curved walls in natural convection, two extensions of the classical boundary-layer theory are discussed: boundary-layer theory of higher order and double-deck theory. Both theories are applied to experiments on a vertical flat plate with humps.

Keywords: flow separation; laminar; natural convection; high-order boundary-layer theory; double-deck theory

Introduction

The calculation of laminar flow in natural convection is usually achieved through the use of the classical boundary-layer theory.¹ This theory, however, cannot predict laminar natural-convection flows with separation, i.e., it cannot predict a zero wall shear stress, as will be shown in Appendix 1. This result is a direct contradiction of experimental evidence. The classical boundary-layer theory is an asymptotic theory, i.e., it represents solutions of the Navier–Stokes and energy equations for high values of the Grashof number. Within the context of this theory, specific terms are neglected that refer to higher-order effects. One of these effects is called the curvature effect, which can be neglected at high Grashof numbers because of the extremely thin boundary layer. Another higher-order effect is the entrainment effect, which induces an external flow that interacts with the boundary layer.

Flow separation can be considered as a higher-order effect in the context of this asymptotic theory. The classical boundary-layer theory can be easily extended to a *boundary-layer theory of higher order*.^{2,3} Moreover, there exists yet a second asymptotic theory for large Grashof numbers, which, in contrast to the boundary-layer theory, treats high values of curvature. This theory has been developed and applied to flows over humps by Merkin⁴ and will be referred to as *double-deck theory* because it involves two layers within the natural-convection flow.

The purpose of the present work is to demonstrate that both theories can predict separation in laminar natural convection. Two different wall geometries will be considered and treated by these theories. The results of both theories will then be compared with experimental results.

Geometric configurations

The first geometry to be considered is a vertical flat plate (see Figure 1) containing a hump whose contour is described by

$$y_s(x) = h \exp \left[-\frac{s}{l} \left(\frac{x}{l} - 1 \right)^2 \right] \quad (1)$$

Here x is the vertical coordinate, h is the height of the hump, and l is the position of the maximum height of the hump. The value s is a measure of the steepness of the hump. It defines the position of the half-maximum height of the hump by the

Address reprint requests to Prof. Gersten at the Institut für Thermo- und Fluidodynamik, Universität Bochum, Fakultät für Maschinenbau, Universitätsstrasse 150, 4630 Bochum 1, Germany.

Received 4 December 1990; accepted 2 April 1991

equation

$$x \left(y_s = \frac{h}{2} \right) = l \left(1 \pm 0.83 \sqrt{\frac{l}{s}} \right) \quad (2)$$

Therefore, flat humps can be characterized by $s/l \rightarrow 0$ and steep humps by $s/l \rightarrow \infty$. As will be seen in the next section, these two limiting cases are represented by the two asymptotic theories: the boundary-layer theory of higher order treats the flat hump well, while the double-deck theory is well suited for the steep humps.

The second geometry is a vertical flat plate containing a semicylinder.

The wall temperature is taken to be constant.

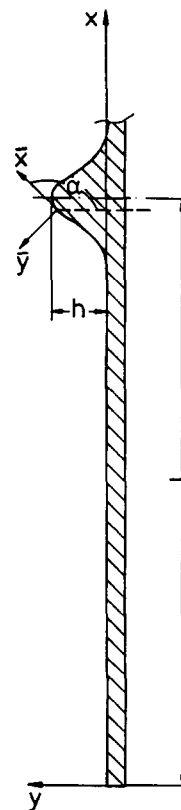


Figure 1 Geometry of vertical flat plate with hump

Theory

Boundary-layer theory of higher order

The continuity equation, the Navier–Stokes equations, and the energy equation are considered in an orthogonal coordinate system, \bar{x} , \bar{y} , where the \bar{x} coordinate follows the contour of the wall as shown in Figure 1. The following dimensionless values are defined:

$$S = \frac{\bar{x}}{l}, \quad N = \frac{\bar{y}}{\varepsilon l}, \quad U = \frac{u}{u_g}, \quad V = \frac{v}{\varepsilon u_g} \quad (3)$$

$$P = \frac{p - p_{stat}}{\rho_\infty u_g^2}, \quad \vartheta = \frac{T - T_\infty}{T_w - T_\infty}$$

with

$$\varepsilon = Gr^{-1/4} \quad (4)$$

$$Gr = \frac{g\beta(T_w - T_\infty)l^3}{\nu^2} = \left(\frac{u_g l}{\nu}\right)^2 \quad (5)$$

$$u_g = \sqrt{g\beta(T_w - T_\infty)l} \quad (6)$$

For the unknown functions, the following asymptotic expansions are assumed:

$$\begin{aligned} U(S, N, \varepsilon) &= u_1(S, N) + \varepsilon[u_{2c}(S, N) + u_{2e}(S, N)] + \dots \\ V(S, N, \varepsilon) &= v_1(S, N) + \varepsilon[v_{2c}(S, N) + v_{2e}(S, N)] + \dots \\ P(S, N, \varepsilon) &= \varepsilon[p_{2c}(S, N)] + \dots \\ \vartheta(S, N, \varepsilon) &= \vartheta_1(S, N) + \varepsilon[\vartheta_{2c}(S, N) + \vartheta_{2e}(S, N)] + \dots \end{aligned} \quad (7)$$

Since the second-order equations are linear, general solutions for these equations can be constructed by adding the curvature-effect terms (index *c*) and entrainment-effect terms (index *e*).

If these expansions are substituted into the flow equations and the individual terms grouped according to the powers of ε , the boundary-layer equations of first and second order are obtained as shown in Appendix 1. The equations representing entrainment are not shown because they correspond to the equations of first order, but have nonzero *u*-components of the velocity at the outer edge of the boundary layer. The system of equations of first order is equivalent to the classical boundary-layer theory.

The variation of the wall shear stress for a particular hump ($h/l=0.097$; $s/l=305$; and the Prandtl number $Pr=6.8$) is shown in Figure 2. The wall shear stress can be described by

$$\frac{\tau_w}{\tau_{w0}} = \frac{\left(\frac{\partial u_1}{\partial N}\right)_w}{\left(\frac{\partial u_0}{\partial N}\right)_w} + \varepsilon \left[\frac{\left(\frac{\partial u_{2c}}{\partial N}\right)_w}{\left(\frac{\partial u_0}{\partial N}\right)_w} + \frac{\left(\frac{\partial u_{2e}}{\partial N}\right)_w}{\left(\frac{\partial u_0}{\partial N}\right)_w} \right] \quad (8)$$

where τ_{w0} is the wall shear stress of the flat plate flow without hump and $(\partial u_0/\partial N)_w$ is the corresponding velocity gradient at the wall. It can be seen that the entrainment effect is negligibly small compared to the curvature effect. According to the first-order theory, the wall shear stress is reduced by not more than 30% just before and just after the hump.

In order to achieve flow separation, τ_w would have to be reduced by an additional 70%. Second-order theory, since it represents only small corrections to first-order theory, will not be able to account for the additional effects in the chosen example. Nevertheless, it does provide the correct qualitative behavior and indicates that separation might occur downstream and eventually even upstream from the maximum height of the hump.

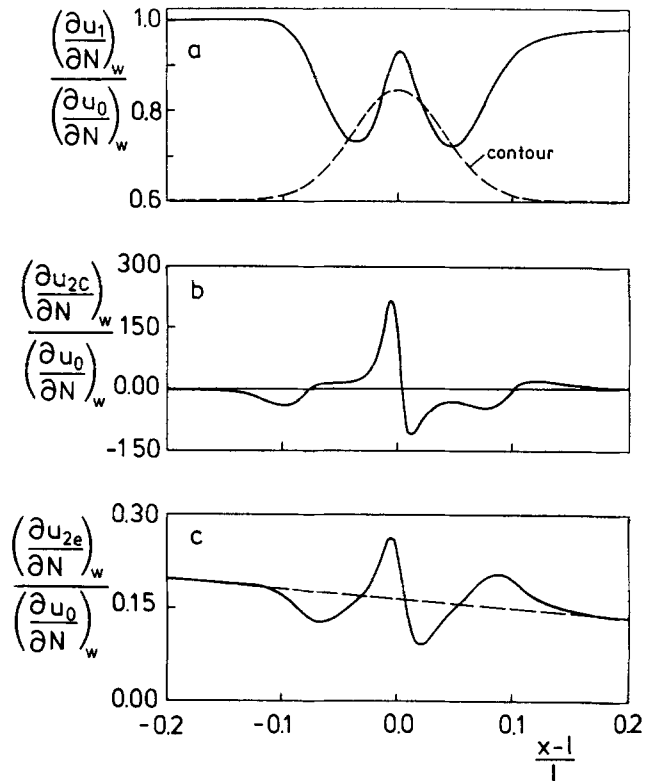


Figure 2 Distributions of wall shear stress for the exponential hump after boundary-layer theory: $h/l=0.097$, $s/l=305$, $Pr=6.8$ (see Equation (8)). (a) First-order theory; (b) second-order effect due to curvature; (c) second-order effect due to entrainment. --- Entrainment of flat plate without hump

Double-deck theory

This theory has been developed by Merkin.⁴ It is similar to the boundary-layer theory discussed above in that it is also an asymptotic theory for $Gr \rightarrow \infty$. In fact, there is a triple-limit process that has to be considered. In addition to $Gr \rightarrow \infty$, $h/l \rightarrow 0$ and $s/l \rightarrow \infty$ are also required with the context that the two dimensionless quantities remain finite:

$$h_M = \frac{h}{l} Gr^{9/28} \gamma^{-1/7} \kappa^{4/7} \quad (9)$$

$$k_M = \sqrt{\frac{s}{l}} Gr^{-3/14} \gamma^{3/7} \kappa^{-5/7} \quad (10)$$

The limiting solution is the vertical flat-plate flow because of $h/l \rightarrow 0$. There is a relationship between the flow parameters and the geometry, i.e., variation of the Grashof number also changes the geometry. The quantities $\gamma(Pr)$ and $\kappa(Pr)$ in Equations (9) and (10) result from the limiting solution for the vertical flat plate and are functions of the Prandtl number (see Appendix 1).

In this limiting solution, there is a layer near the wall (inner deck) in which the velocity and temperature distribution can be replaced by their tangents at the wall. The relationship between the flow parameters and the geometry results from the requirement that the height of the hump is of the order of the thickness of this wall layer. This requirement creates a two-layer structure to this flow. The properties of the two decks are as follows.

Inner deck. The thickness of this layer represents the height of the hump and is of the order of $O(Ge^{-9/28})$. The length in the

flow direction is $O(Gr^{-6/28})$. A result of this particular scaling is that the buoyancy forces can be neglected in comparison to the inertial, pressure, and viscous forces, i.e., the momentum equation is uncoupled from the energy equation. The pressure is independent of the distance from the wall and is impressed on the inner deck from the outer deck. The major influence of the inner deck is to displace the outer deck. This displacement results in a pressure field in the outer deck that then acts on the inner deck.

It will be shown in Appendix 2 that the equations for the inner deck are given by the classical boundary layer without buoyancy but satisfying specific boundary conditions of the given problem. The results are the distributions of heat flux and shear stress at the wall. The latter is given by

$$\frac{\tau_w}{\tau_0} = \left(\frac{\partial u_i}{\partial y_i} \right)_w \quad (11)$$

where τ_0 is the wall shear stress of the flat-plate flow at the plate center ($\tau_0 = \tau_{w0}(x/l = 1)$).

Outer deck. The thickness of the outer deck is of the same order as that of the boundary layer without a hump, namely, $O(Gr^{-1/4})$. The length is the same as in the inner deck, $O(Gr^{-6/28})$. The flow in the outer deck consists of the flow on a vertical flat plate along the hump contour and a small correction. The equations for the correction can be so drastically reduced that explicit local solutions can be given. Here again, the flow field is uncoupled from the temperature field. In particular, the momentum equation in the y -direction yields a simple relationship between the wall pressure and the displacement function $A(x_i)$:

$$P_w(x_i) = -A''(x_i) \quad (12)$$

with

$$x_i = \gamma^{-3/7} \kappa^{5/7} \varepsilon^{-6/7} \frac{x-l}{l} \quad (13)$$

The most important function of the outer deck is the buildup of a pressure field resulting from the displacement of the inner deck.

Comparison of the two theories

The natural-convection flow over a vertical plate with a hump can be characterized by four dimensionless quantities:

- Grashof number Gr
- Prandtl number Pr
- Relative height of hump h/l
- Relative steepness of hump s/l

Instead of the Grashof number, the relative boundary-layer thickness, δ/l , for flat-plate flow without hump can be used, since

$$\frac{\delta}{l} = \varepsilon = Gr^{-1/4} \quad (14)$$

Both asymptotic theories are valid for the following limits at a given Prandtl number:

Boundary-layer theory: $\delta/l \rightarrow 0 (Gr \rightarrow \infty), h/l \rightarrow 0, s/l \rightarrow 0, h/\delta \rightarrow \infty$

Double-deck theory: $\delta/l \rightarrow 0 (Gr \rightarrow \infty), h/l \rightarrow 0, s/l \rightarrow \infty, h/\delta \rightarrow 0$

The theories are different based on their regions of validity with regard to s/l and h/δ .

Hence, the two theories are valid for different ranges of the parameters, as shown schematically in Figure 3. If (as in the

case of forced convection³) one differentiates between local and massive separation depending on whether the hump height is very large or very small compared with the boundary-layer thickness, the double-deck theory can describe only local separation, whereas the boundary-layer theory describes the massive separation.

Experiment

Experiments were performed in a water tank with the two wall configurations described above. A nearly two-dimensional (2-D) (plane) flow could be established in this test facility. The wall was heated to only 0.25 K above the temperature of the undisturbed fluid in order to provide laminar flow over the entire length of the wall configuration. The flow velocity in the free convective flow was measured with a white-light speckle method.⁵ This method allows the resolution of the sign of the flow-velocity vectors, and it can therefore detect possible areas of separated and reversed flow. The error in the measurements was estimated to be less than 3%.

The plate with the hump contour based on Equation (1) had the following characteristics:

$$l = 155 \text{ mm} \quad T_w = 21.51^\circ\text{C}$$

$$h = 15 \text{ mm}$$

$$s = 47.3 \text{ m} \quad T_\infty = 21.26^\circ\text{C}$$

The corresponding dimensionless parameters are given by

$$Gr = 2.1 \cdot 10^6 (\varepsilon = \delta/l = 0.026), \quad Pr = 6.8$$

$$h/l = 0.097, \quad h/\delta = 3.73, \quad s/l = 305$$

The plate with the semicylinder hump had the following characteristics:

$$l = 155 \text{ mm} \quad Gr = 2.1 \cdot 10^6$$

$$R = 19 \text{ mm} \quad Pr = 6.8$$

$$\delta/R = \delta/h = 0.21$$

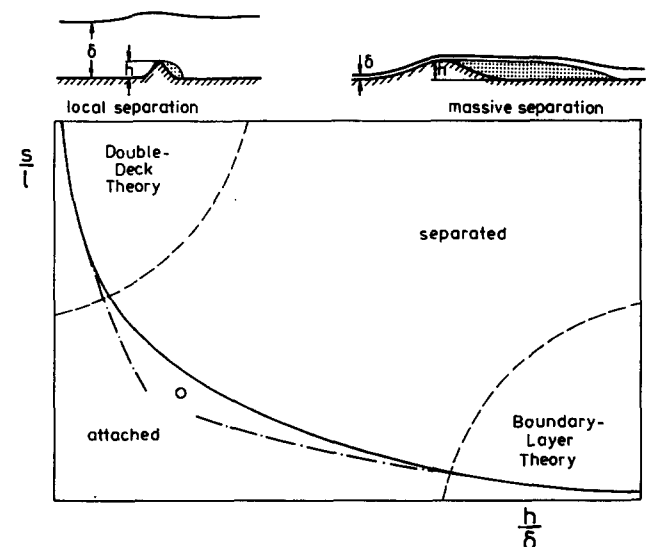


Figure 3 Schematic parameter diagram with areas of validity for the two asymptotic theories ($Gr = \text{const} \gg 1$). — Boundary between attached and separated flows. - - - Asymptotes for asymptotic theories. ○ Experimental point for exponential hump. - - - Areas of validity of the theories

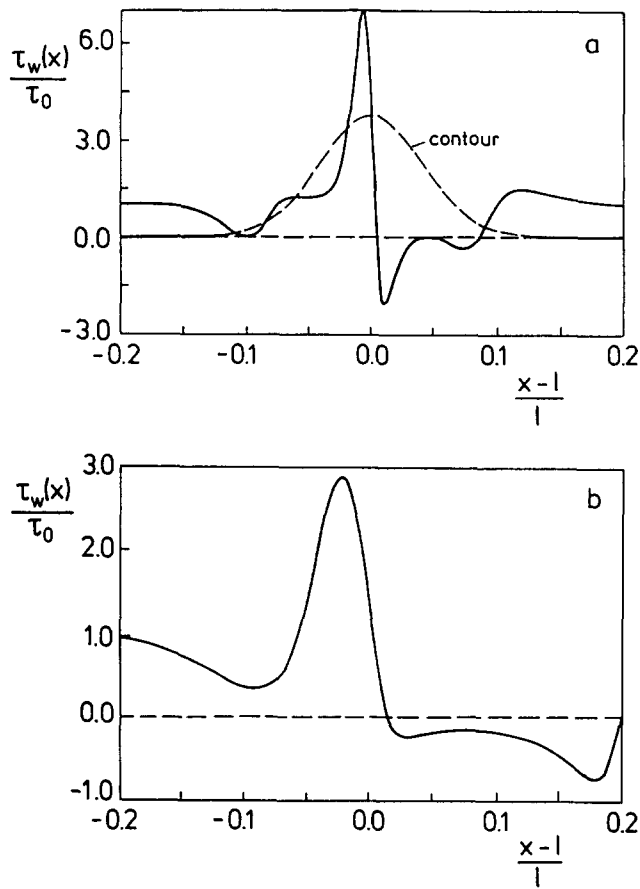


Figure 4 Distributions of wall shear stress for the exponential hump ($Gr = 2.1 \cdot 10^6$; $\epsilon = Gr^{-1/4} = 0.026$; $Pr = 6.8$; $h/l = 0.097$; $s/l = 305$). (a) Boundary-layer theory; (b) double-deck theory

Results and discussion

Exponential hump

The experimental parameters $\epsilon = 0.026$ and $h/l = 0.097$ are sufficiently small to be considered asymptotic. More problematic is the value of $s/l = 305$, which appears large (double-deck theory) rather than small (boundary-layer theory).

Figure 4 shows the variation of the wall shear stress based on the two theories. Separation occurs in both cases, although the length of the separation region is twice as long in the double-deck theory as in the boundary-layer theory. But it is worth mentioning that in spite of the different streamwise scales of the separated regions, there exists a similar character of the wall shear-stress distributions. There is a rapid decrease in wall shear stress at separation, followed by a region where τ_w is fairly flat, with a final sharp dip in τ_w before reattachment.

Figure 5 shows that relatively weak separation occurs, as can be seen in the boundary between the attached and separated flows. Figure 5a is valid for the value $s/l = 305$, and Figure 5b for the value $h/l = 0.097$.

When $s/l = 305$, the double-deck theory ($s/l \rightarrow \infty$) is more likely to be valid. The experimental value, as shown in Figure 5a, is very close to the boundary between flows without and with separated regions.

In fact, the measurements on the vertical plate with a hump have shown that areas of local flow separation cannot be verified within the limits of accuracy of the method. The relatively low velocities in this type of flow could be measured in areas not closer than 1 mm from the wall. Here the velocity

had dropped to a value (0.2 mm/s) below which velocities could not be resolved. The experiment has been conducted with a finite value of the Grashof number and, therefore, separated flow may exist in the narrow regime at 1 mm from the wall.

Semicylinder hump

The infinitely large curvature that occurs at the intersection between the flat plate and the cylindrical hump makes it questionable whether either theory is appropriate for this case. The boundary-layer theory is valid only for boundaries with small curvature.

The double-deck theory can be formally applied to this case, but the discontinuity in the contour makes it necessary to analyze the results with caution, particularly near the corners.

With the aforementioned considerations, calculations have been carried out that are shown in Figure 6. The experimentally

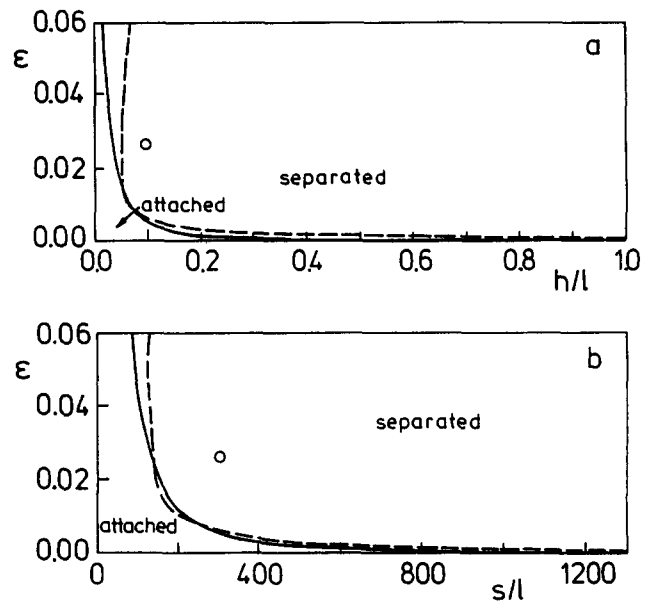


Figure 5 Boundary between attached flows and flows with separation. (a) $s/l = 305$; (b) $h/l = 0.097$. — Boundary-layer theory. - - - Double-deck theory. o Experiment ($\epsilon = 0.026$; $h/l = 0.097$; $s/l = 305$)

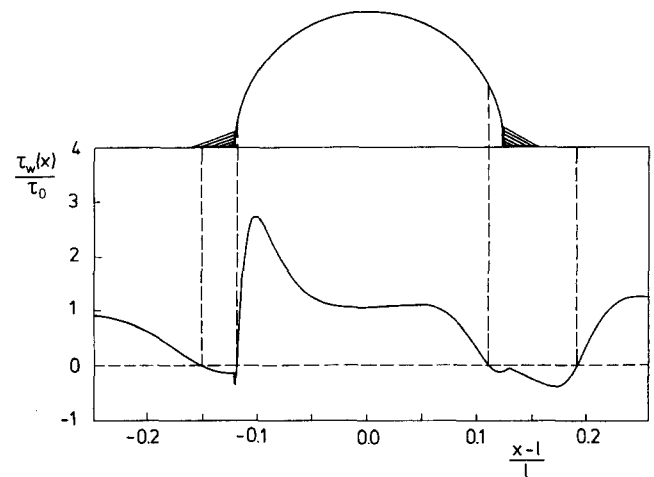


Figure 6 Distribution of wall shear stress for the flat plate with semicylinder according to double-deck theory. //// Areas of separated flow observed by experiments

determined separation regions are shown in relation to the hump contour as shaded areas. The experiments show clearly the existence of dead-water regimes in the corner regions of the semicylinder configuration. These dead-water regions in which the flow velocity is nominally zero can be taken as areas of separated flow with negligible flow reversal. The extension of these areas is in qualitative agreement with the results of the double-deck calculations.

Summary

The classical boundary-layer theory cannot determine separation on curved walls in natural convection because separation is a higher-order effect. Two extensions of the classical boundary-layer theory are discussed: boundary-layer theory of higher order and double-deck theory. Both theories were applied to experiments on a vertical flat plate with humps.

Both theories are asymptotic theories for $Gr \rightarrow \infty$, $h/l \rightarrow 0$, and $h/\delta \rightarrow \infty$ (boundary-layer theory) and $h/\delta \rightarrow 0$ (double-deck theory). Although the experimental configurations were both outside of the region of validity of the theories, there was qualitative agreement. In the case of the exponential hump, both theories predicted weak separation, but this could not be verified by the experiments. In the case of the semicylinder hump, experimental results showed separation in the corners, which was predicted by the double-deck theory.

Acknowledgment

The investigations have been financially supported by Ministerium für Wissenschaft und Forschung des Landes Nordrhein-Westfalen, Düsseldorf (Projects Nr. IV A 5-FA 9992 and IV B 5-FA 9992).

References

- 1 Schlichting, H. *Grenzschichttheorie*, Verlag Braun, Karlsruhe, 1982
- 2 Gersten, K. and d'Avila, J. S. Higher order boundary-layer effects in combined free and forced convection. ESA-TT-498, 1979, 122-131
- 3 Gersten, K. Die Bedeutung der Prandtlischen Grenzschichttheorie nach 85 Jahren. *Z. Flugw. Weltraumforsch. Bd.*, 1989, 13, 209-218
- 4 Merkin, J. A. Free convection boundary layers over humps and indentations. *Q. J. Mech. Appl. Math.*, 1983, 36, 71-85
- 5 Grobel, M. and Merzkirch, W. Measurement of natural convection by speckle velocimetry. *Laser Institute of America (LIA)*, 1988, 63, 97-99

Appendix 1: Flow equations for the higher-order boundary-layer theory

First order

$$\frac{\partial u_1}{\partial S} + \frac{\partial v_1}{\partial N} = 0$$

$$u_1 \frac{\partial u_1}{\partial S} + v_1 \frac{\partial u_1}{\partial N} = \vartheta_1 \sin \alpha + \frac{\partial^2 u_1}{\partial N^2}$$

$$u_1 \frac{\partial \vartheta_1}{\partial S} + v_1 \frac{\partial \vartheta_1}{\partial N} = \frac{1}{Pr} \frac{\partial^2 \vartheta_1}{\partial N^2}$$

The boundary conditions at the wall as described below give

$$N=0: \left(\frac{\partial^2 u_1}{\partial N^2} \right)_w = -\sin \alpha < 0 \quad \text{for } 0 < \alpha < \pi$$

whereas $(\partial^2 u_1 / \partial N^2)_w > 0$ is a necessary condition for the separation point.

From the first-order solution for the flat plate ($\alpha = \pi/2$) at $x=l$ ($S=S_0$), one gets

$$\gamma(Pr) = \int_0^\infty u_0(S_0, N) dN, \quad \kappa(Pr) = \left(\frac{\partial u_0}{\partial N} \right)_{w,s_0}$$

$$\Lambda(Pr) = \left(\frac{\partial \vartheta_0}{\partial N} \right)_{w,s_0}$$

For $Pr=6.8$, this leads to $\gamma=0.13$, $\kappa=0.64$, $\Lambda=-0.74$.

Second order

$$\frac{\partial u_{2c}}{\partial S} + \frac{\partial v_{2c}}{\partial N} = 0$$

$$u_1 \frac{\partial u_{2c}}{\partial S} + u_{2c} \frac{\partial u_1}{\partial S} + v_1 \frac{\partial u_{2c}}{\partial N} + v_{2c} \frac{\partial u_1}{\partial N} = \vartheta_{2c} \sin \alpha - \frac{\partial p_{2c}}{\partial S} + \frac{\partial^2 u_{2c}}{\partial N^2}$$

$$+ k \left(N \frac{\partial^2 u_1}{\partial N^2} + \frac{\partial u_1}{\partial N} - N v_1 \frac{\partial u_1}{\partial N} - u_1 v_1 + N \vartheta_1 \sin \alpha \right)$$

$$k u_1^2 = -\vartheta_{2c} \cos \alpha + \frac{\partial p_{2c}}{\partial N}$$

$$u_1 \frac{\partial \vartheta_{2c}}{\partial S} + u_{2c} \frac{\partial \vartheta_1}{\partial S} + v_1 \frac{\partial \vartheta_{2c}}{\partial N} + v_{2c} \frac{\partial \vartheta_1}{\partial N} = \frac{1}{Pr} \frac{\partial^2 \vartheta_{2c}}{\partial N^2}$$

$$+ k \left[-N v_1 \frac{\partial \vartheta_1}{\partial N} + \frac{1}{Pr} \left(\frac{\partial^2 \vartheta_1}{\partial N^2} + \frac{\partial \vartheta_1}{\partial N} \right) \right]$$

where $k(S) = -\frac{d\alpha}{dS}$.

Boundary conditions

$$N=0: \quad u_1 = v_1 = \vartheta_1 - 1 = u_{2c} = v_{2c} = \vartheta_{2c} = 0$$

$$N \rightarrow \infty: \quad u_1 = \vartheta_1 = u_{2c} = \vartheta_{2c} = p_{2c} = 0$$

Appendix 2: Flow equations for the inner deck of double-deck theory⁴

$$\frac{\partial u_i}{\partial x_i} + \frac{\partial v_i}{\partial y_i} = 0$$

$$u_i \frac{\partial u_i}{\partial x_i} + v_i \frac{\partial u_i}{\partial y_i} = -\frac{dP_w}{dx_i} + \frac{\partial^2 u_i}{\partial y_i^2}$$

$$u_i \frac{\partial \vartheta_i}{\partial x_i} + v_i \frac{\partial \vartheta_i}{\partial y_i} = \frac{1}{Pr} \frac{\partial^2 \vartheta_i}{\partial y_i^2}$$

$$P_w(x_i) = -A''(x_i)$$

Boundary conditions

$$x_i \rightarrow -\infty: \quad A=0, u_i = y_i, \vartheta_i = y_i$$

$$y_i = 0: \quad u_i = v_i = \vartheta_i = 0$$

$$y_i \rightarrow \infty: \quad u_i = y_i + y_{ci}(x_i) + A(x_i)$$

$$\vartheta_i = y_i + y_{ci}(x_i) + A(x_i)$$

where

$$y_i = \gamma^{-1/7} \kappa^{4/7} \left(\frac{y-y_c}{l} \right) e^{-9/7}$$

$$x_i = \gamma^{-3/7} \kappa^{5/7} \frac{x-l}{l} e^{-6/7}$$

$$u_i = \gamma^{-1/7} \kappa^{-3/7} u_1 e^{-6/7}$$

$$v_i = \gamma^{2/7} \kappa^{-4/7} v_1 e^{2/7}$$

$$\vartheta_i = \gamma^{-1/7} \kappa^{4/7} \Lambda^{-1} (\vartheta_1 - 1) e^{-6/7}$$

$$y_{ci} = h_M \exp(k_M x_i)^2$$